Polymer Chemistry

ROYAL SOCIETY OF CHEMISTRY

PAPER

View Article Online
View Journal | View Issue

Cite this: *Polym. Chem.*, 2025, **16**, 4261

Facile synthesis and properties of thioamide-containing polymers

Hongqing Zhang, Huazhang Wang, Longgang Xia, Xinghao Du and Chun Feng *

Polythioamide, a variant of polyamide in which the carbonyl oxygen atom is replaced with sulfur, shows stronger metal affinity, weaker hydrogen-bonding interactions with water, and higher refractive indices in comparison with its counterpart polyamide. The development of efficient, versatile and economical strategies to prepare polythioamides along with gaining much deeper insights into their structure–property relationships, is crucial for creating new polythioamide-based functional materials. In this work, we describe a convenient and efficient platform to generate a variety of polythioamides. The commodity polymers poly(*N*-isopropylacrylamide) (PNIPAM), poly(*N*,*N*-dimethylacrylamide) (PDMA), poly(vinylpyrrolidone) (PVP) and polyurethane (PU), which have high-volume and low-cost production, can be readily thionated using commercially available Lawesson reagent to convert the amides to thioamides in a controlled manner with negligible chain degradation or crosslinking. For thionated PNIPAM, a higher level of thionation leads to a higher glass transition temperature and a lower decomposition temperature. The thionation of PNIPAM decreases its solubility in water. The LCST of thionated PNIPAM with 16% thioamide content decreases to 13 °C, and thionated PNIPAM with ≥44% thioamide content cannot be dissolved in water at temperatures as low as 0 °C. The addition of the metal ions Ag^+, $AuCl_4^-$ and Hg^{2+} increases the solubility of thionated PNIPAM owing to the strong coordinating capacity of thioamides toward Ag^+, $AuCl_4^-$ and Hg^{2+}. Metal nanoparticles, for example, Ag and Au nanoparticles, can be embedded in thionated PU foams, which can be employed as reusable catalysts for the reduction of 4-nitrophenol to 4-aminophenol. This study provides an efficient and versatile platform and important guidelines for developing thioamide-containing polymers for diverse applications.

Received 24th July 2025,
Accepted 26th August 2025

DOI: 10.1039/d5py00737b

rsc.li/polymers

Introduction

The development of new polymer materials with desirable properties/functionalities remains a persistent and highly attractive focus in polymer chemistry and materials science.[1] Most polymers are composed of only C, H, O and N with diverse chemical structures. The introduction of other elements, such as S, Si, P and Fe, can significantly alter the properties of polymers.[2–5] In particular, the introduction of S atoms into a polymer can endow the resulting polymer materials with many interesting features, such as high refractive indices, metal complexation ability, redox activity, and self-healing capacity.[6,7] Thus, the development of new synthetic routes for the efficient and facile preparation of S-containing polymers has attracted growing attention.[8]

To date, "bottom-up" and postfunctionalization strategies have been developed for the preparation of S-containing polymers.[9–15] In the "bottom-up" strategy, the polymerization or copolymerization of S-containing monomers, including dithiols, carbonyl sulfide (COS), carbon disulfide (CS_2), monothiodilactone, episulfides and S_8, is a widely used route to synthesize S-containing polymers.[9] For example, Bowman *et al.* reported the synthesis of various S-containing polythiolethers *via* thiol–ene, thiol-Michael or thiol-epoxy reactions using dithiols as key reagents.[10,11] Ren and co-workers reported the preparation of semicrystalline poly(monothiocarbonate)s *via* the copolymerization of COS and ethylene oxide, an achiral epoxide, using a chromium-containing complex as a catalyst.[12] Diebler *et al.* reported the copolymerization of epoxides with CS_2 to give S-containing polymers containing both monothiocarbonate and trithiocarbonate linkages using LiO^tBu as the initiator.[13] Tao and co-workers reported the preparation of poly(monothiodilactone) with an M_n of up to 120 kDa *via* the organocatalyzed ring-opening polymerization of monothiodilactone.[14] Pyun and co-workers reported the preparation of S-containing polythiolethers from S_8 and various olefinic monomers *via* inverse vulcanization.[15] Hu, Tang and Ren *et al.* also reported the synthesis of a variety of polythioamides and other S-containing polymers *via* multicomponent reactions

Shanghai Key Laboratory of Advanced Polymeric Materials, School of Materials Science and Engineering, East China University of Science and Technology, 130 Meilong Road, Shanghai 200237, People's Republic of China.
E-mail: cfeng@ecust.edu.cn; Tel: +86-21-54925606

from S_8, diamines, diisocyanides, alkynes, carbonyl chlorides and other sources.[16–19] Despite these significant advances in preparing S-containing polymers, most approaches still require moisture-sensitive monomers and precious catalysts. This highlights the need for more robust, cost-efficient and versatile preparation methods.

The postfunctionalization strategy provides an alternative platform to prepare S-containing polymers. Postfunctionalization approaches are usually based on the incorporation of S-containing moieties into S-free polymers.[20] In particular, to leverage the appealing high-volume and low-cost production of commodity polymers, the polymer science community has become interested in the preparation of S-containing polymers with diverse structures/functionalities from commodity polymers *via* the postfunctionalization strategy.[21] Thioether-containing polymers can be readily prepared from the commodity polymers polybutylene (PB) and polyisoprene (PI), as well as PB- and PI-containing copolymers, through thiol–ene chemistry by using the vinyl groups of PB/PI as handles.[22,23] In addition to the thioether group, thioamide is another interesting S-containing unit. Thioamides are a variant of amides in which the carbonyl oxygen atom is replaced with a sulfur atom; they have much lower oxidation potentials, higher affinities for metals, and higher rotational barriers around the C–N bonds in comparison with their amide counterparts.[24,25] Owing to the lower oxidation potential and higher rotational barrier of thioamide, the replacement of amides with thioamides could be a method to regulate the solubility, luminescence, and pharmacokinetics of thioamide-containing peptides and proteins.[26–32] In addition, taking advantage of the higher metal affinity of thioamides, thioamide-containing polymers have been used to efficiently recycle Au^{3+} and Hg^{2+} ions.[33,34] Given the interesting properties of thioamide-containing materials, it is important to develop efficient methods to prepare thioamide-containing polymers from commodity polymers and obtain deeper insight into how the thioamide moiety influences the properties of thioamide-containing polymers.

Lawesson reagent (2,4-bis(4-methoxyphenyl)-2,4-dithioxo-1,3-dithiadiphosphetane, LR) has been widely used to convert amide units to thioamides in organic synthesis.[35] In 1990, Levesque and Deletre reported the first example of the preparation of various thioamide-containing polymers from the polyamides polyamide-6, polyamide-11 and poly(ether-*block*-amide) through the thionation of amide units using LR, along with a limited investigation of their properties, such as UV/vis absorption and viscosity measurements.[36] Recently, Luxenhofer and co-workers reported the preparation of thioamide-containing polymers from poly(2-ethyl-2-oxazoline) (PEtOx) using LR for the thionation of amides.[26] In this work, the influence of the proportion of thioamide units on the glass transition temperatures, thermal stability and low critical solution temperature (LCST) of the resulting thionated PEtOx was investigated. Inspired by these works, we herein report the preparation of a series of thioamide-containing polymers from the commercially available (commodity) polymers poly(*N*-isopropylacrylamide) (PNIPAM), a well-known thermo-responsive polymer, poly(*N*,*N*-dimethylacrylamide) (PDMA), poly(vinylpyrrolidone) (PVP) and polyurethane (PU), by using LR for the thionation of amides (Scheme 1). Thionation of PNIPAM was found to reduce its solubility and lower the LCST. The addition of the metal ions Ag^+, $AuCl_4^-$ and Hg^{2+} significantly increased the solubility of the thionated PNIPAM, owing to the strong coordination of thioamides with Ag^+, $AuCl_4^-$ and Hg^{2+}. Interestingly, thionated PU foam can be embedded with either Ag or Au nanoparticles, which can be used as recyclable catalysts for the reduction of 4-nitrophenol to 4-aminophenol (Scheme 1B).

Results and discussion

Thionation with Lawesson reagent

Lawesson reagent (LR) has been widely used for thionation in organic synthesis to access thioamides.[35] However, reports on the usage of this interesting and efficient reagent in polymer modification to prepare thioamide-containing polymers from polyamides remain limited.[35,36] Herein, we first tested the thionation of PNIPAM, a well-known thermo-responsive polymer with a lower critical solution temperature (LCST) of around 33 °C in water, as a model sample with the LR. To this end, PNIPAM (M_n = 20 800 g mol^{-1}, $Đ$ = 1.88, 0.75 g mL^{-1} in $CHCl_3$) was treated with LR with molar feeding ratios of LR to repeat units of PNIPAM ([LR]/[NIPAM]) of 0.25, 0.50, 0.75 and 1.00 at 60 °C for 24 h (Fig. 1A). After purification, the resulting products were subjected to gel permeation chromatography (GPC), elemental analysis, and ^{1}H and ^{13}C nuclear magnetic resonance (NMR) and Fourier transform infrared (FT-IR) spectroscopies. First, elemental analysis of S showed that the weight contents of S (C_S) were 4.4%, 11.6%, 18.6% and 20.4% for the molar feeding ratios of 0.25, 0.50, 0.75 and 1.00, respectively (Table 1). Based on the results obtained from elemental analysis, the molar contents of C═S units ($C_{C=S}$) were calculated to be about 16%, 43%, 72% and 80% for the samples PNIPAM-S16, PNIPAM-S43, PNIPAM-S72 and PNIPAM-S80 obtained using molar feeding ratios of 0.25, 0.50, 0.75 and 1.00, respectively (Table 1). One can note the appearance of the typical peaks a′ at 4.02 ppm and a at 4.60 ppm, which are attributed to the –C*H*NHCO– and C*H*NHCS– protons, respectively, in the ^{1}H NMR spectra of the products after the thionation (Fig. 1B), indicative of the substitution of O of C═O units with S. Based on the integral ratios of peak a to peak a′, the efficiency of the substitution of the O of the C═O units with S, that is, the molar content of C═S units ($C_{C=S}$), was estimated to be about 22%, 50%, 71% and 79% for the molar feeding ratios of 0.25, 0.50, 0.75 and 1.00, respectively (Fig. 1B and Table 1), which are in good agreement with the values obtained from elemental analysis. In the ^{13}C NMR spectrum of the product with a feeding ratio of 0.25 (Fig. 1C), the peak a′ at 175 ppm corresponds to the C of the –NHCO– units, while the peak a at 210 ppm is attributed to the C of –NHCS– units. For the sample with a feeding ratio of 1.00, the peak a at 210 ppm remained, but the peak a′ disappeared (Fig. 1C). These obser-

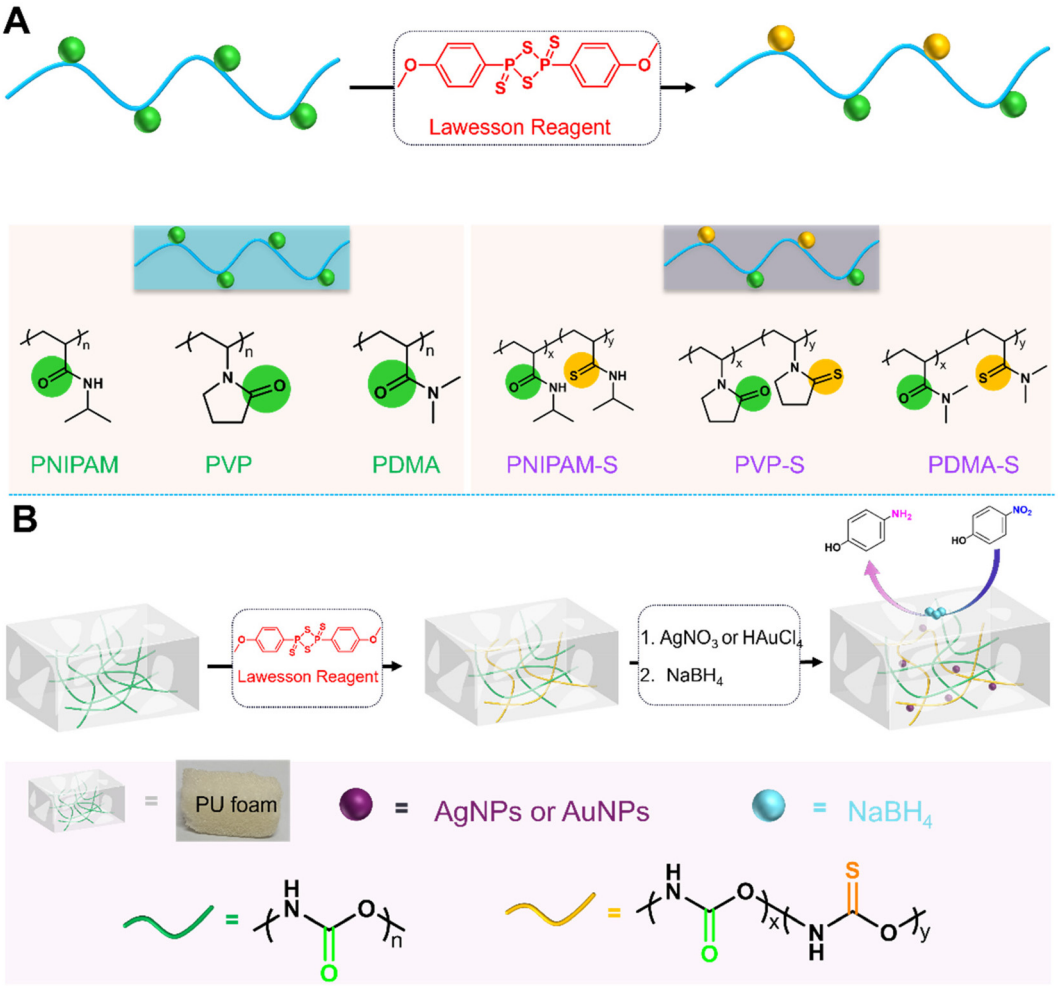

Scheme 1 Schematic illustrations of the preparation of (A) thioamide-containing polymers from PNIPAM, PDMA and PVP, and (B) Ag- and Au-nanoparticle-coated thioamide-containing PU foams used as recyclable catalysts for the reduction of 4-nitrophenol to 4-aminophenol.

vations further indicated that the higher the [LR]/[NIPAM] ratio, the higher the efficiency of the substitution of O with S. All the products gave monomodal eluent peaks with eluent times comparable to that of pristine PNIPAM without any shoulders at much shorter or longer eluent times (Fig. 1D), indicative of the absence of chain crosslinking or scissoring during the thionation reaction. This notion was further supported by the observation that the pristine PNIPAM and all the products have comparable apparent molecular weights. It was found that the typical peaks at 1432 cm^{-1} attributed to the vibration of –NHCS– groups appeared in the FT-IR spectra of the resulting products, and the intensities of these peaks increased with increasing feeding ratio (Fig. 1E). All these results revealed that the C═O units of PNIPAM can be transformed into C═S groups using LR, and that the content of C═S units can be regulated *via* the feeding ratio of [LR]/[NIPAM].

Thermal properties of thionated PNIPAM

We then examined the influence of the content of C═S units on the thermal properties of thionated PNIPAM using differential scanning calorimetry (DSC) and thermogravimetric analysis (TGA) (Fig. 2). From the DSC curves of the resulting thionated PNIPAM, one can note that the glass transition temperature (T_g) values of thionated PNIPAM were higher than that of the pristine PNIPAM (145 °C). For example, the T_g values of thionated PNIPAM-S16, PNIPAM-S43, PNIPAM-S72 and PNIPAM-S80 were 150 °C, 157 °C, 162 °C and 165 °C, respectively, indicative of the increased T_g for thionated PNIPAM with a higher content of C═S units. Previous reports have shown that the T_g of polymers was dependent on their chain flexibility, especially the backbone rotational flexibility.[26,37] Given the much larger size of the S atom in comparison with the O atom, we inferred that the transformation of C═O units into C═S units would lead to an increase in the rotational barrier of the C–C bonds of the backbones linking the C═S units.

TGA analysis revealed that the 5% weight loss temperatures ($T_{deg,5\%}$) of pristine PNIPAM and thionated PNIPAM-S16, PNIPAM-S43, PNIPAM-S72 and PNIPAM-S80 were about 363 °C, 339 °C, 318 °C, 301 °C and 280 °C, respectively, demonstrating the decreased thermal stability of thionated

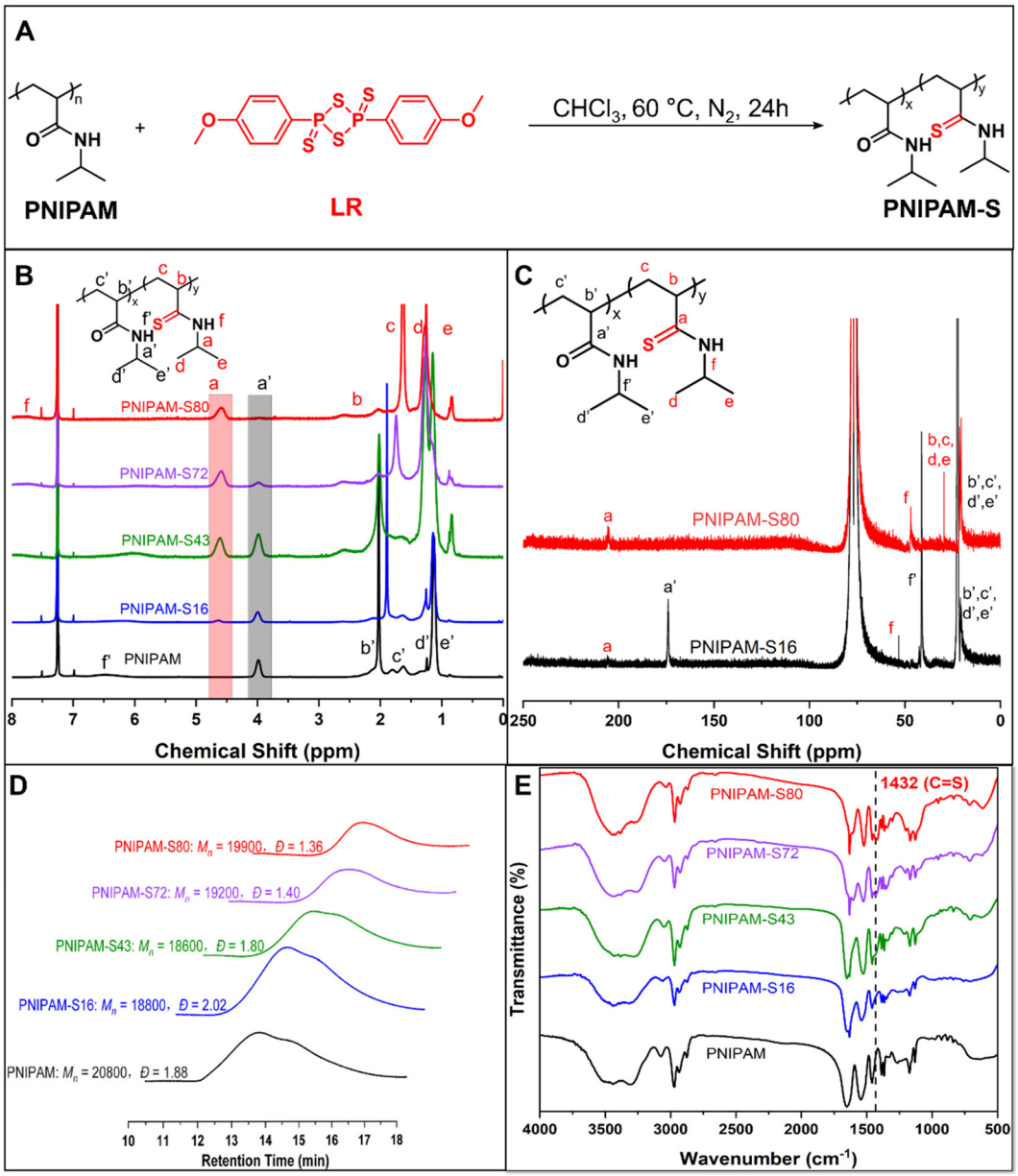

Fig. 1 (A) Schematic illustration of the thionation of PNIPAM with LR. (B) ^{1}H NMR spectra, (D) GPC curves and (E) FT-IR spectra of pristine PNIPAM and thionated PNIPAM with molar feeding ratios of 0.25, 0.50, 0.75 and 1.00. (C) ^{13}C NMR spectra of thionated PNIPAM with feeding ratios of 0.25 and 1.00.

Table 1 Characteristics of thionated PNIPAM obtained under different conditions[a]

Sample	[LR]/[NIPAM]	C═S content[b] (%, from ^{1}H NMR)	*S* weight content (%, from EA)	C═S content[c] (%, from EA)	M_n[d] (KDa)	*Đ*[d]	T_g[e] (°C)	$T_{deg.5\%}$[f] (°C)
PNIPAM	—	—	—	—	20.8	1.88	145	363
PNIPAM-S16	0.25	22	4.4	16	18.8	2.02	150	339
PNIPAM-S43	0.50	50	11.6	43	18.6	1.80	157	318
PNIPAM-S72	0.75	71	18.6	72	19.2	1.40	162	301
PNIPAM-S80	1.00	79	20.4	80	19.9	1.36	165	280

[a] The reaction was performed in $CHCl_3$ at 60 °C for 24 h. [b] The C═S contents ($C_{C=S}$) were obtained based on integral ratios of peaks a and a′ in Fig. 1B ($C_{C=S} = I_a/(I_a + I_{a'}) \times 100\%$). [c] The C═S contents ($C_{C=S}$) were obtained based on *S* weight contents measured *via* elemental analysis ($C_{C=S} = 113C_S/(32 - 16C_S) \times 100\%$). [d] M_n and *Đ* values were obtained *via* GPC using THF as the eluent and PS as standards. [e] T_g values were obtained based on DSC analysis. [f] $T_{deg.5\%}$ values were obtained based on TGA analysis.

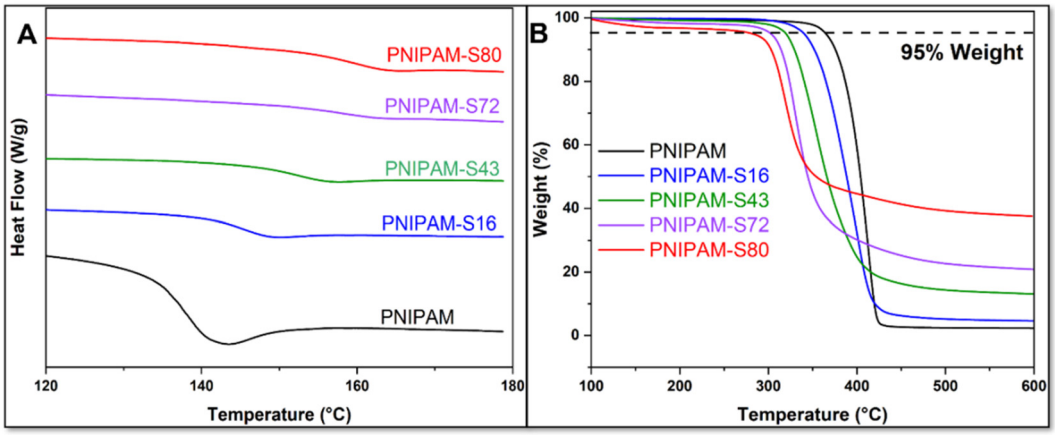

Fig. 2 (A) DSC and (B) TGA curves of pristine PNIPAM and PNIPAM-S16, PNIPAM-S43, PNIPAM-S72 and PNIPAM-S80.

PNIPAM with a higher content of C═S units. This phenomenon was in agreement with previous reports,[26,38] which showed that thionation reduced the thermal stability of naphthalene diimide-bithiophene copolymers and poly(2-ethyl-2-oxazoline) owing to the relatively lower thermal stability of thioamindes compared to amides. In addition, the residual mass at 600 °C increased with the increasing content of C═S units in the thionated PNIPAM, consistent with the increase in S weight content in the thionated PNIPAM measured using elemental analysis (Table 1).

Solution behavior of thionated PNIPAM

PNIPAM is a widely used thermo-responsive polymer that exhibits an LCST of ~33 °C in aqueous media.[39–42] The chemical structure and composition of PNIPAM are important factors influencing its LCST.[43–46] The influence of the level of thionation on the solution behavior of thionated PNIPAM in water was then examined.

First, it was found that the solubility of PNIPAM significantly decreased after thionation. Only the sample PNIPAM-S16 was soluble in cold water, while the other samples (PNIPAM-S43, PNIPAM-S72 and PNIPAM-S80) with higher levels of thionation were insoluble in cold water (~0 °C). This phenomenon indicated increased hydrophobicity at higher levels of thionation, which is consistent with a previous report on the thionation of poly(2-ethyl-2-oxazoline).[26]

Turbidimetry measurements of the aqueous solution of PNIPAM-S16 (1.0 mg mL^{-1}) showed that a transparent solution was obtained when the temperature was below 14 °C, and the solution immediately became cloudy when the temperature exceeded 15 °C (Fig. 3A). As the temperature was further elevated to from 16 °C to 40 °C, the transmittance slowly decreased from 96% to 86% (Fig. 3A). DLS analysis revealed that the apparent hydrodynamic diameter ($D_{h,app}$) of PNIPAM-S16 was about 20 nm at 10 °C (Fig. 3B), at which it was likely in a unimolecular state. As the temperature increased from 10 °C to 15 °C, the $D_{h,app}$ increased to about 60 nm, indicating the formation of aggregates. The $D_{h,app}$ flocculated around 60 nm as the temperature further increased from 15 °C to 38 °C. The trend was consistent with the variation of the count rate with the temperature (Fig. 3B). On the contrary, the aqueous solution of PNIPAM (1.0 mg mL^{-1}) exhibited typical temperature-responsive behavior with an LCST of ~33 °C (Fig. 3A). These observations indicated that

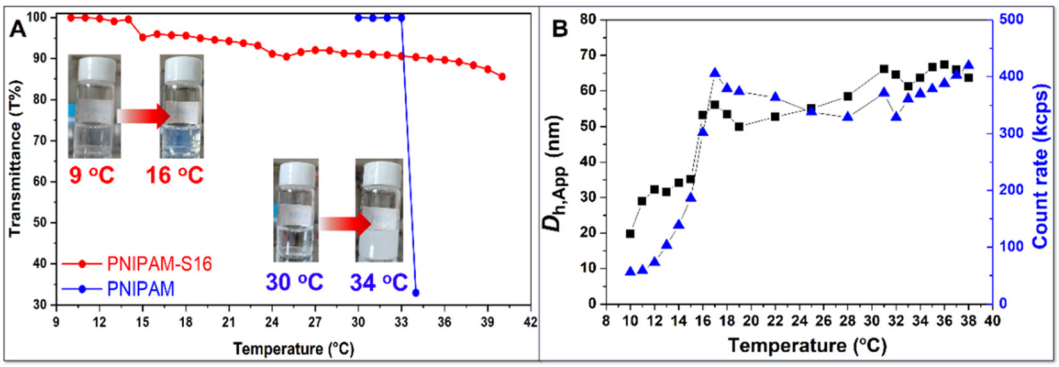

Fig. 3 (A) Transmittance of aqueous solutions of PNIPAM and PNIPAM-S16 (1.0 mg mL^{-1}, λ = 500 nm). (B) Dependence of $D_{h,app}$ and count rate of the aqueous solution of PNIPAM-S16 (1.0 mg mL^{-1}) on temperature.

the thionated PNIPAM-S16 started to aggregate when the temperature was above about 15 °C to form micelles containing a "CHNHCS"-rich core and "CHNHCO"-rich corona (Fig. 4), which exhibited different solution behavior than PNIPAM. Of note, the transmittance of the solution of PNIPAM-S16 did not show as significant a decrease as that of the solution of pristine PNIPAM (Fig. 3A). Although the "CHNHCO"-rich domains should become insoluble above 33 °C, the aggregation of micelles did not occur, likely owing to the relatively small size of the micelles (~60 nm) and low concentration of PNIPAM-S16 (1.0 mg mL^{-1}).

To obtain more information regarding the solution behavior of PNIPAM-S16, ^{1}H NMR spectra of PNIPAM-S16 in D_2O (5.0 mg mL^{-1}) were recorded at different temperatures (Fig. 4). At 9 °C, the characteristic peaks of PNIPAM-S16, including peak a at 3.65 ppm, attributed to the protons of the –C*H*NHCS– units and peak a′ at 4.26 ppm, attributed to the proton of the –C*H*NHCO– units were observed. This observation indicated that PNIPAM-S16 was in a unimolecular state in D_2O at 9 °C, in agreement with the DLS results (Fig. 3B). As the temperature was elevated from 9 °C to 13 °C, the peaks a and a′ seemed to attenuate slightly. As the temperature was increased to 14 °C, peak a almost completely disappeared, with an obvious decrease in peak a′. Of note, despite the disappearance of peak a attributed to the proton of the –C*H*NHCS– units at 16 °C, peak a′ assigned to the proton of the –C*H*NHCO– units was still visible, indicative of the presence of "soluble" PNIPAM domains without thionation. These observations indicated that the increase in temperature showed a much more significant influence on the "CHNHCS"-rich domains than the "CHNHCO"-rich domains. In this regard, we inferred that the collapse/aggregation of PNIPAM-S16 chains with increasing temperature was mainly due to the decrease in solubility of the "CHNHCS"-rich domains.

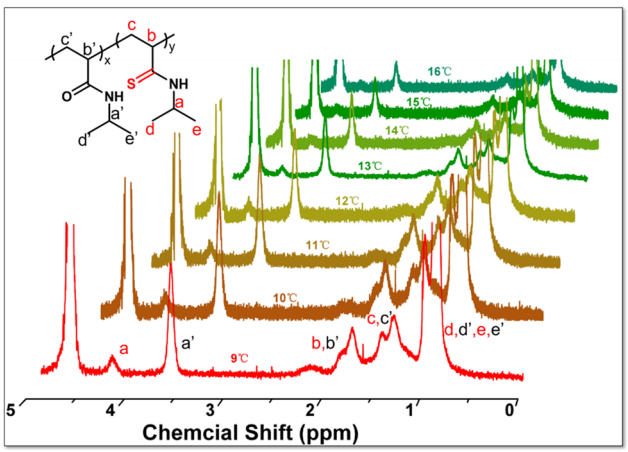

Fig. 4 ^{1}H NMR spectra of PNIPAM-S16 in D_2O (5.0 mg mL^{-1}) at different temperatures.

Previous works on sulfur-containing polymers showed that S-containing polymers were endowed with metal coordination capacity.[33,47–51] We thus further examined the influence of metal ions on the solubility of thionated PNIPAM. Aqueous solutions of PNIPAM-S16 (1.0 mg mL^{-1}) containing 0.5 molar equivalent of NaCl, $Zn(CH_3COO)_2$, $MgSO_4$, $Hg(CF_3SO_3)_2$, $AgNO_3$ of $HAuCl_4$ relative to the thioamide (C═S) units of PNIPAM-S16 ([M]/[C═S] = 0.5) all remained transparent at 0 °C (Fig. S1A), showing that PNIPAM-S16 was soluble in the presence of these salts. At 14 °C, the solution of PNIPAM-S16 in the absence of any salt was cloudy, whereas visible aggregates appeared in the solutions containing NaCl, $Zn(CH_3COO)_2$ and $MgSO_4$ (Fig. S1B), likely owing to the salting-out effect. Turbidimetry measurements showed that the aggregates were formed above around 14 °C for these solutions (Fig. 5B). In stark contrast, the solutions of PNIPAM-S16 containing $Hg(CF_3SO_3)_2$ remained transparent without noticeable aggregation even when the temperature was elevated from 0 °C to 40 °C (Fig. 5C). These phenomena indicated that $Hg(CF_3SO_3)_2$, $AgNO_3$ and $HAuCl_4$ significantly improved the solubility of PNIPAM-S16. Of note, the PNIPAM exhibited comparable LCST values in both the absence and presence of NaCl, Zn

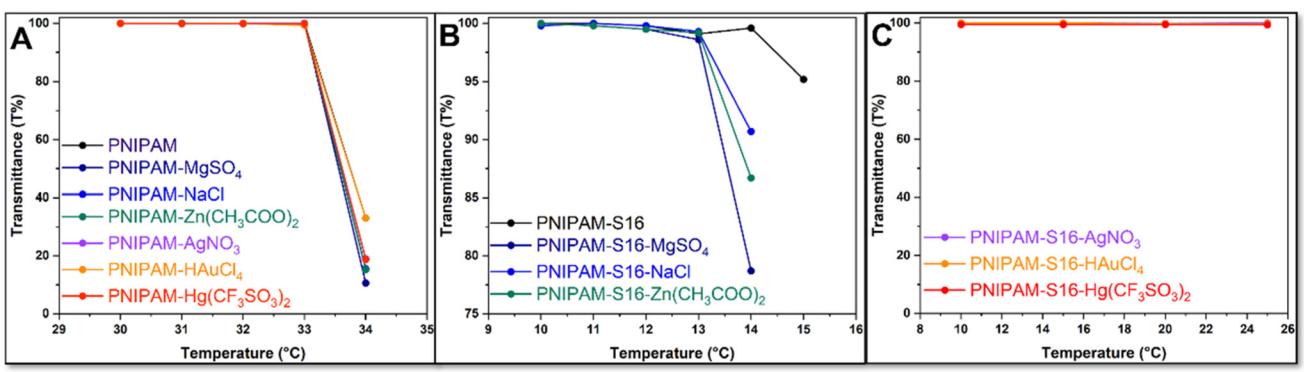

Fig. 5 Transmittance of aqueous solutions of (A) PNIPAM (1.0 mg mL^{-1}, λ = 700 nm) containing NaCl, $Zn(CH_3COO)_2$, $MgSO_4$, $Hg(CF_3SO_3)_2$, $AgNO_3$ and $HAuCl_4$. Transmittance of aqueous solutions of PNIPAM-S16 (1.0 mg mL^{-1}, λ = 700 nm) containing (B) NaCl, $Zn(CH_3COO)_2$ and $MgSO_4$ and (C) $Hg(CF_3SO_3)_2$, $AgNO_3$ and $HAuCl_4$.

$(CH_3COO)_2$, $MgSO_4$, $Hg(CF_3SO_3)_2$, $AgNO_3$ and $HAuCl_4$ (Fig. 5A and S1C, D), indicative of the negligible influence of these salts on the solubility of PNIPAM. These observations showed that the thionated PNIPAM was endowed with interesting metal-ion-dependent solubility behavior.

To obtain more information regarding the different metal-ion-dependent solubility behavior of PNIPAM and thionated PNIPAM, solutions of PNIPAM and PNIPAM-S16 in D_2O (5 mg mL^{-1}) with and without $AgNO_3$ were then subjected to ^1H NMR analysis (Fig. 6). For the PNIPAM solutions with and without $AgNO_3$, the characteristic peaks of the protons originating from PNIPAM appeared in the ^1H NMR spectra at 20 °C, and almost disappeared at 40 °C (Fig. 6A), demonstrating the typical thermo-responsive solution behavior of PNIPAM with an LCST of around 33 °C. For the solution of PNIPAM-S16 without $AgNO_3$, peaks a and a′ originating from the protons of –C*H*NHCO– and –C*H*NHSO– appeared at 4 °C and almost disappeared at 20 °C (Fig. 6B), in agreement with the observations in the above turbidimetry measurements (Fig. 3A). Interestingly, for the solution of PNIPAM-S16 containing $AgNO_3$, the peak attributed to the proton of –C*H*NHCS– disappeared at 4 °C (Fig. 6B), likely indicative of the coordination of C═S units to Ag^+ ions. In addition, the other typical peaks attributed to the protons of PNIPAM-S16 showed negligible variation as the temperature was elevated from 4 °C to 20 °C (Fig. 6B), which showed that PNIPAM-S16 was well dissolved at 20 °C in the presence of $AgNO_3$. This phenomenon was consistent with the observations in the turbidimetry measurements (Fig. 5C). All the above-described results revealed that the Ag^+ had almost no effect on the solubility of PNIPAM, but significantly increased the solubility of PNIPAM-S16 in water. We inferred that the different solution behavior of PNIPAM and thionated PNIPAM was likely due to the coordination of C═S units with Ag^+ ions.

To further verify the coordination of C═S units with Ag^+ ions, both aqueous solutions of PNIPAM (M_n = 20 800 g mol^{-1}, $Đ$ = 1.88, 0.10 mg mL^{-1}) and PNIPAM-S16 (M_n = 18 800 g mol^{-1}, $Đ$ = 2.02, 0.10 mg mL^{-1}) were incubated with $AgNO_3$ (0.0015 mg mL^{-1}) at 25 °C for 24 h, respectively. Subsequently, the solutions were subjected to ultrafiltration using a membrane with a molecular weight cutoff of 3 kDa, which is much lower than the M_n of PNIPAM and PNIPAM-S16 (Fig. 7A). The contents of Ag^+ ions in the solutions before ultrafiltration ($C_{0,Ag}$) and in the obtained filtrates ($C_{F,Ag}$) were then measured using inductively coupled plasma optical emission spectroscopy (ICP OES). It was supposed that the Ag^+ coordinated with the polymers (PNIPAM or PNIPAM-S16), which have molecular weights much higher than 3 kDa (the molecular weight cutoff of the membrane) could not penetrate the membrane, and that only free Ag^+ that was not coordinated with the polymers would be able to penetrate the membrane. The fraction of Ag^+ ($P_{P\text{-}Ag}$) that could penetrate the membrane was estimated using the values of $C_{0,Ag}$ and $C_{F,Ag}$ ($P_{P\text{-}Ag} = C_{F,Ag}/C_{0,Ag}$). It was found that the $P_{P\text{-}Ag}$ for the solution of PNIPAM-S16 was about 22% (Fig. 7B), which was about 43% lower than that of the solution of PNIPAM (65%). The significantly lower penetration capacity of Ag^+ in the solution of PNIPAM-S16 compared to that in the solution of PNIPAM indicated the much higher coordinating capacity of PNIPAM-S16 with Ag^+.

We then further evaluated the coordinating capacity of PNIPAM-S16 with different metal ions using the above-described approach. It was found that the values of $P_{P\text{-}Au}$ and $P_{P\text{-}Hg}$ were about 16% and 20%, which were similar to the value of $P_{P\text{-}Ag}$. In contrast, the values of $P_{P\text{-}Pt}$, $P_{P\text{-}Na}$, $P_{P\text{-}Zn}$ and $P_{P\text{-}Mg}$ were about 77%, 84%, 81% and 86%, respectively (Fig. 7C). These results revealed that the PNIPAM-S16 was endowed with much higher coordinating capacities toward Ag^+, $AuCl_4^-$ and Hg^{2+} than toward Pt^{2+}, Na^+, Zn^{2+} and Mg^{2+},

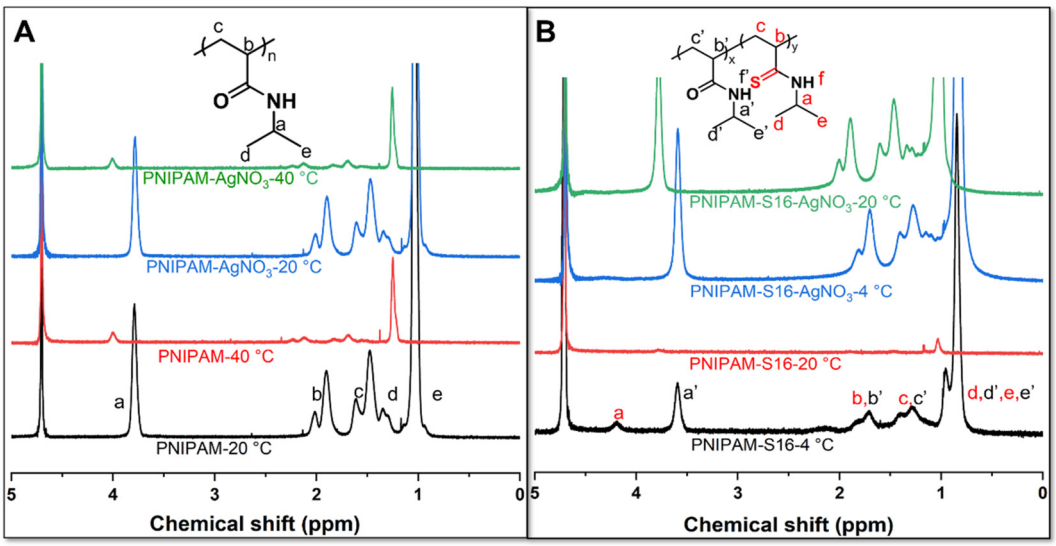

Fig. 6 ^1H NMR spectra of (A) PNIPAM and (B) PNIPAM-S16 in D_2O (5.0 mg mL^{-1}) with and without $AgNO_3$ at different temperatures.

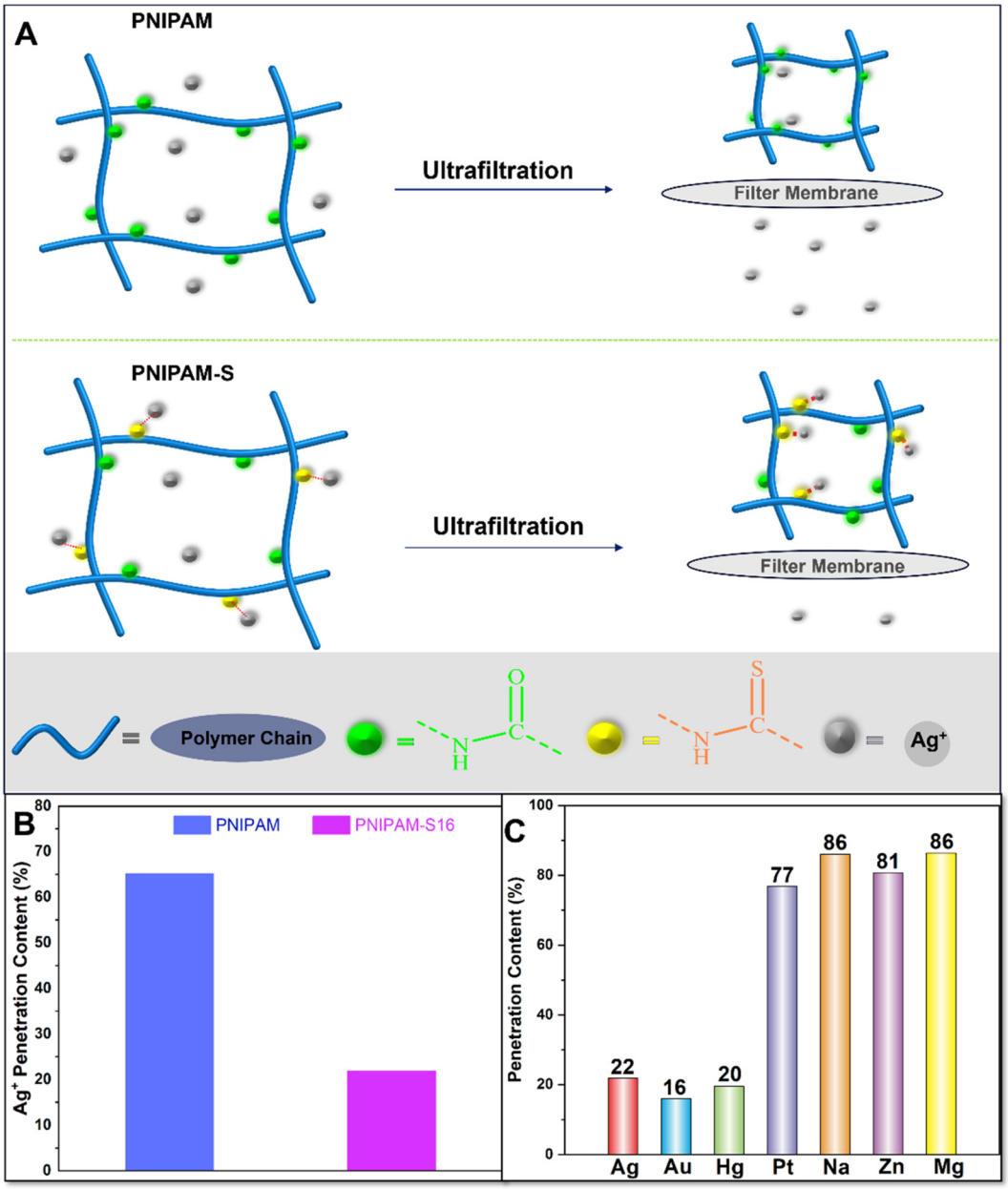

Fig. 7 (A) Schematic illustration of the capture of Ag^+ by PNIPAM and thionated PNIPAM. (B) Histograms of the contents of remaining Ag^+ in the filtrates for PNIPAM and PNIPAM-S16. (C) Histograms of the contents of remaining metal ions in the filtrates of solutions of PNIPAM-S16.

which was consistent with the observations of different metal-ion-dependent solution behaviors for thionated PNIPAM-S16 (Fig. 5). The distinct affinities of PNIPAM-S16 toward different metal ions can be interpreted on the basis of Pearson's soft–hard acid–base (SHAB) theory,[34,52] which states that a soft base exhibits much higher affinity toward a soft acid than a hard acid and *vice versa*. C═S is regarded as a soft base, which is more prone to coordinate to the soft acids Ag^+, $AuCl_4^-$ and Hg^{2+}, than the hard acids Na^+, Zn^{2+} and Mg^{2+} and the borderline acid Pt^{2+}.[34,52] This notion can be supported by the distinct solubility product constants (K_{sp}) of S-based salts, which reflect the affinity of S toward metal ions. For example, the K_{sp} values of HgS and Ag_2S are 4.0×10^{-53} and 6.0×10^{-51}, respectively, which are much lower than those of ZnS (2.9×10^{-25}).[34]

All these results demonstrated that the thionation of PNIPAM *via* the substitution of the O of C═O groups with S significantly affected (decreased) the solubility (LCST) of thionated PNIPAM in water. In addition, the thionated PNIPAM with C═S units was endowed with much higher coordinating capacity toward Ag^+, $AuCl_4^-$ and Hg^{2+} ions than toward Pt^{2+}, Na^+, Zn^{2+} and Mg^{2+}, and thus, thionated PNIPAM exhibited more pronounced metal-ion-dependent solubility behavior than PNIPAM.

Extension of the thionation strategy to other amide-containing polymers

Based on the interesting thermal and solution properties of thionated PNIPAM, we then attempted to extend the thionation strategy to other amide-containing polymers. Commercially available polyvinylpyrrolidone (PVP, M_n = 21 900 g mol^{-1}, $Đ$ = 1.96) and poly(*N*,*N*-dimethyl acrylamide) (PDMA, M_n = 10 200 g mol^{-1}, $Đ$ = 2.63) were each treated with LR using different molar feeding ratios (Fig. 8A). In the ^{1}H NMR spectra of thionated PVP (Fig. 8B), new peaks a′ and d′ at 4.76 ppm appeared alongside the characteristic peaks of PVP a and d at 3.28 and 3.72 ppm, indicating the thionation of –C═O– units in PVP. It was found that the integral ratios of the peaks a′ and d′ to the peaks a and d increased with increasing feeding ratio (Fig. 8B), showing an increase in the level of thionation with increasing feed ratio. This notion was supported by the increase of the intensity of the peak at 1493 cm^{-1} corresponding to the C═S units of thionated PVP and the attenuation of the peak at 1663 cm^{-1} corresponding to C═O units with increasing feeding ratio (Fig. 8C). From the GPC curves of the resulting thionated PVP (Fig. 8D), it was found that all the thionated PVP had monomodal peaks comparable with the pristine PVP, showing the absence of chain crosslinking and degradation during the thionation reaction. Similarly, thionation also occurred on PDMA to give thionated PDMA with controlled levels of thionation (Fig. S2). These results demonstrated the versatility of the thionation strategy for the preparation of thioamide-containing polymers using LR.

Surface functionalization of thionated commercial polyurethane foam

Given the excellent coordinating ability of C═S units with some interesting metal ions,[33,47–51] for example, Ag^+ and $AuCl_4^-$, the thionated polymers could be used for fabricating functional polymer/metal hybrid materials. In a proof-of-concept experiment, a piece of commercially available polyurethane (PU) foam was treated with LR, aiming to thionate the C═O units of PU to give PU-S (Fig. 9A). Subsequently, the resulting foam PU-S was immersed in an aqueous solution of $AgNO_3$ for incubation for 3 h at 25 °C, allowing the introduction of Ag^+ ions onto the surface of the thionated PU-S foam. Then, the resulting foam was further immersed in a solution of $NaBH_4$ to immobilize Ag nanoparticles onto the surface of the thionated PU-S foam *via in situ* reduction of the Ag^+ ions. In a control experiment, a piece of PU foam that had not

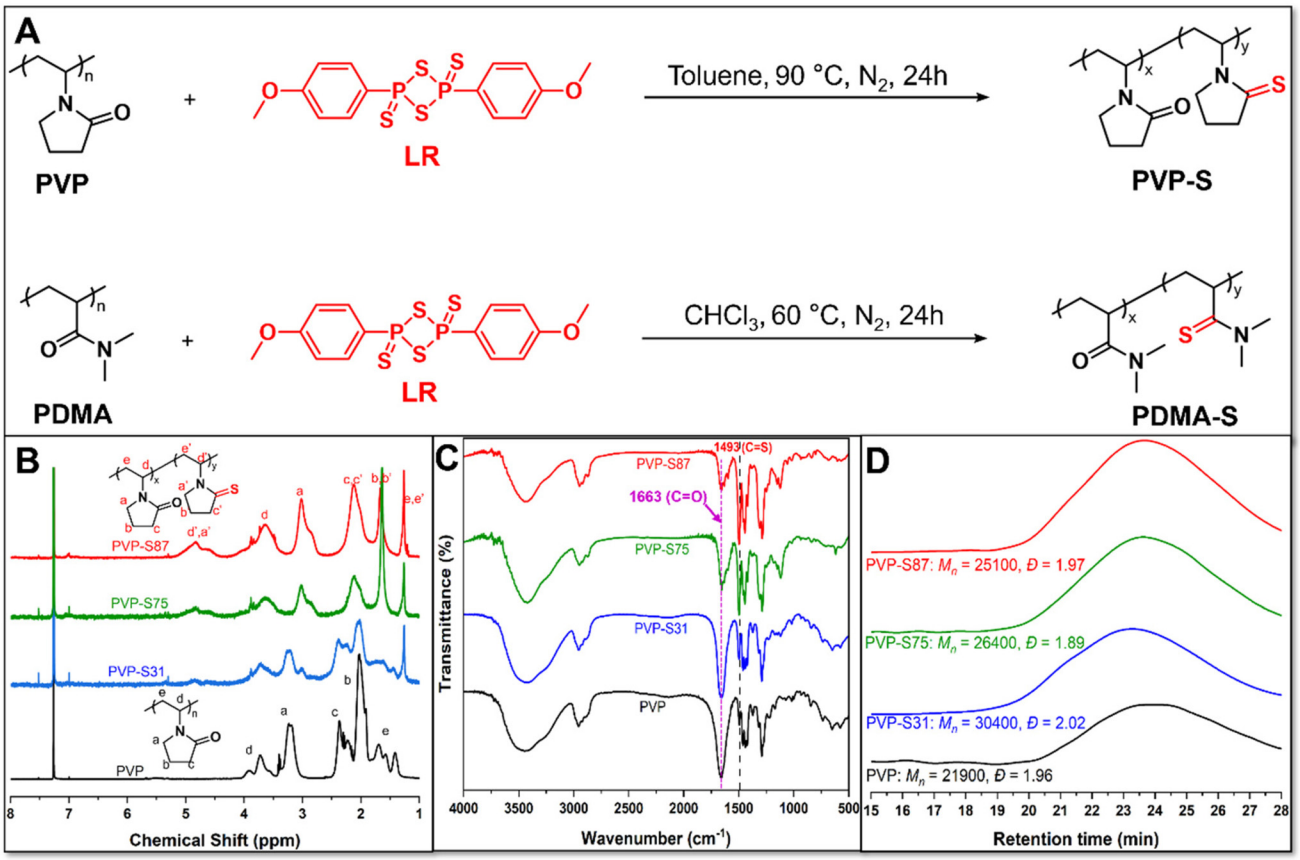

Fig. 8 (A) Schematic illustration of the thionation of PVP and PDMA. (B) ^{1}H NMR spectra, (C) FT-IR spectra and (D) GPC curves of pristine PVP and thionated PVP with feeding ratios of 0.25, 0.50, and 1.00.

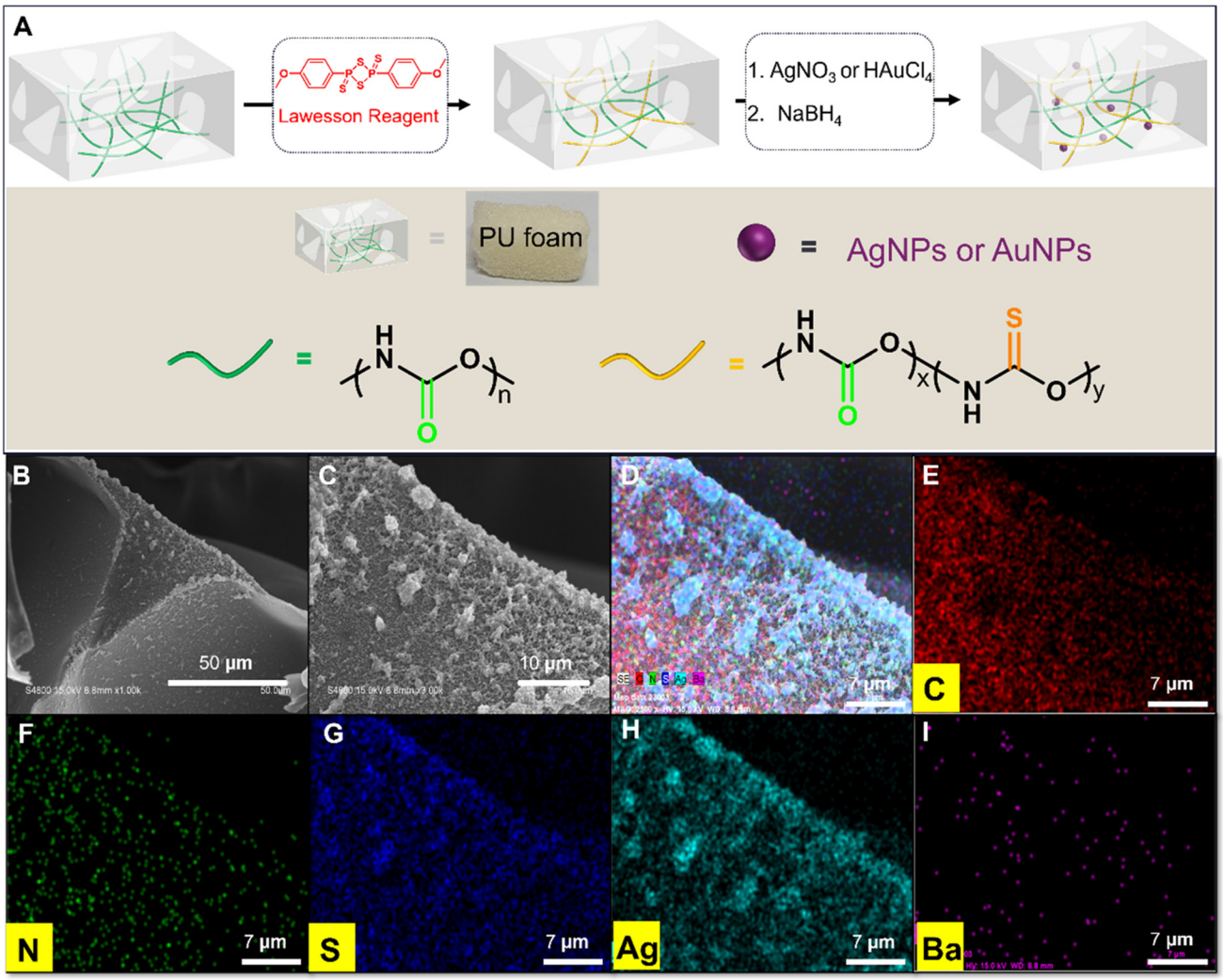

Fig. 9 (A) Schematic illustration of the thionation of PU foam, surface functionalization of the thionated PU-S foam with AgNPs and AuNPs. SEM images of (B) thionated PU-S foam and (C) thionated PU-S foam coated with AgNPs. Elemental mappings of (E) C, (F) N, (G) S, (H) Ag and (I) Ba on the thionated PU-S foam coated with Ag nanoparticles and (D) overlay of the elements of C, N, S and Ag from (E) to (H).

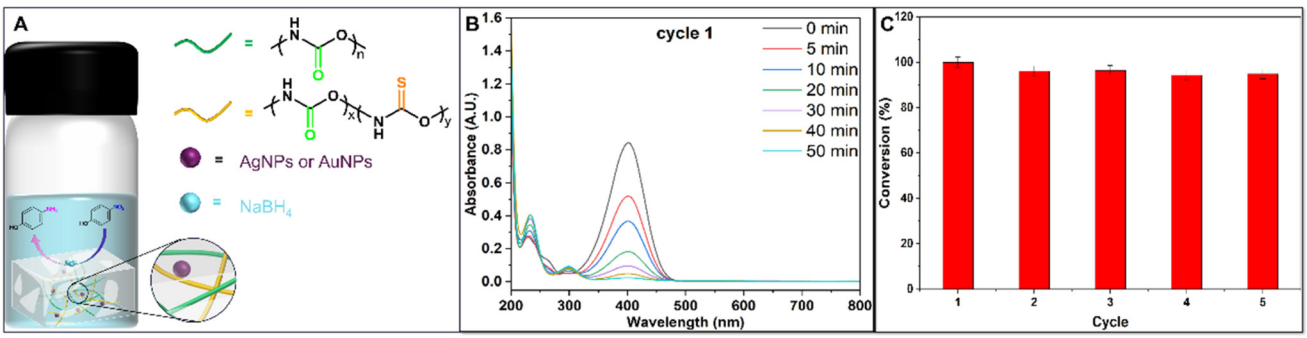

Fig. 10 (A) Schematic illustration of the reduction of 4-nitrophenol into 4-aminophenol using thionated PU-S foams coated with AgNPs and AuNPs as recyclable catalysts. (B) UV/vis absorption spectra of 4-nitrophenol solutions with the immersed PU-S foam coated with AgNPs in the first cycle of reaction. (C) Conversion of 4-nitrophenol over five cycles using thionated PU-S foam coated with AgNPs as a recyclable catalyst.

undergone thionation was directly treated with $AgNO_3$, followed by the treatment with $NaBH_4$ using the same protocol.

It was found that the PU foam turned from light yellow to dark yellow after the thionation (Fig. S3). On the contrary, the PU foam that did not undergo the thionation did not show such variation. Additionally, scanning electronic microscopy (SEM) analysis revealed that the surface of the PU-S foam became much rougher with abundant irregular particles (Fig. 9B and C). In addition, mapping of C, N, S, O, Ag and Ba *via* energy dispersive X-ray spectroscopy (EDX) analysis revealed that the surface of the PU-S foam was rich in the elements C, N, S, O and Ag in comparison with Ba, which was used as a negative control (Fig. 9D–I). These observations indicated the occurrence of the thionation of the PU-S foam using LR and the immobilization of Ag nanoparticles (AgNPs) onto the surface of the thionated PU-S foam.

Of note, the resulting thionated foam coated with AgNPs exhibited catalytic activity for the complete reduction of 4-nitrophenol into 4-aminophenol in 60 min (Fig. 10A and B). On the contrary, the PU foam prepared without thionation showed negligible catalytic activity under the same conditions (Fig. S4), indicative of the presence of only a few AgNPs on the PU foam. These results further indicated that the C═O units of PU foam can be thionated to give thioamide-containing PU-S foam, and AgNPs can be further immobilized onto the surface of the thionated PU-S foam by leveraging the high coordinating ability of C═S units with Ag^+ ions. More importantly, the thionated foam embedded with AgNPs can be easily recycled. The PU-S foam coated with AgNPs was then used in four subsequent cycles of reduction reactions. The results showed that all four reactions proceeded smoothly with conversions above 95% in 60 min (Fig. 10C and S5). The AgNPs appeared to be tightly embedded on the surface of the thionated PU-S foam with only marginal release of AgNPs from the thionated PU-S foam indicated by the slight decrease in the conversion and apparent rate constant in consecutive reactions (Fig. S6). Similarly, AuNPs can also be immobilized onto thionated PU-S foam for the repeated reduction of 4-nitrophenol (Fig. S7 and 8). These results demonstrated that the thionated polymers could be used for the generation of functional hybrid polymer/metal materials.

Conclusion

In summary, we reported the preparation of a variety of thioamide-containing polymers from commercially available polyamides, such as PNIPAM, PVP, PDMA and PU, by using LR to convert amides into thioamides in a controlled manner without either chain degradation or crosslinking. The content of thioamide can be regulated by the feeding ratio of LR to amides. Using PNIPAM as a model sample, it was found that the T_g of thionated PNIPAM increased, but its thermal stability decreased, with increasing content of thioamide units. The thionation of PNIPAM decreased its water solubility. Thionated PNIPAM with 16% of thioamides showed an LCST of 15 °C, and thionated PNIPAM with thioamide contents above 43% exhibited limited solubility in cold water at 0 °C. However, the coordination of the C═S units of thionated PNIPAM with Ag^+, $AuCl_4^-$ and Hg^{2+} increased the solubility of the thionated PNIPAM in water. Owing to the high affinity of C═S units toward Ag^+ and $AuCl_4^-$, Ag and Au nanoparticles can be incorporated onto the surface of thionated PU foam. The resulting thionated PU foam coated with AgNPs and AuNPs can be used as a reusable catalyst for the reduction of 4-nitrophenol into 4-aminophenol. Given the high efficiency and versatility of LR chemistry, along with the large-scale, low-cost production of commodity polyamides, this study offers a facile and economical platform for constructing thioamide-containing functional polymer materials for diverse applications.

Author contributions

HQZ – investigation and formal analysis. HZW, LGX and XHD – investigation. CF – conceptualization, resources and funding acquisition. All authors-review and editing.

Conflicts of interest

The authors declare no competing financial interests.

Data availability

The data, including figures and tables, supporting this article have been included as part of the SI.

Supplementary information: Polymer synthesis and characterization, procedures of sample preparation. See DOI: **https://doi.org/10.1039/d5py00737b**.

Acknowledgements

The authors are thankful for financial support from National Natural Science Foundation of China (U22A20131 and 52361165657).

References

1 Z. Y. Zhang, Y. H. Wang, H. Zhou, H. B. Dai, J. J. Luo, Y. Z. Chen, Z. L. Li, M. D. Li, C. Li, E. L. Gao, K. Jiao and J. Zhang, *Adv. Fiber Mater.*, 2025, **7**, 774–783.
2 Y. Hu, L. Zhang, Z. Wang, R. Hu and B. Z. Tang, *Polym. Chem.*, 2023, **14**, 2617–2623.
3 Z. He, H. Zhang, J. Xie, T. Zhou and J. Zhang, *Eur. Polym. J.*, 2024, **221**, 113570.
4 X. Solimando, E. Kennedy, G. David, P. Champagne and M. F. Cunningham, *Polym. Chem.*, 2020, **11**, 4133–4142.

5 H. Liu, Y. Zhang, Y. B. Li, N. Han, H. H. Liu and X. X. Zhang, *Adv. Fiber Mater.*, 2024, **6**, 772–785.
6 X. Zhou, Y. Cui, X. Xun, J. Jia, X.-C. Wang and Z.-J. Quan, *Sep. Purif. Technol.*, 2025, **365**, 132679.
7 D. Fan, D. Wang, J. Zhang, X. Fu, X. Yan, D. Wang, A. Qin, T. Han and B. Z. Tang, *J. Am. Chem. Soc.*, 2024, **146**, 17270–17284.
8 P. Sang, Q. Chen, D.-Y. Wang, W. Guo and Y. Fu, *Chem. Rev.*, 2023, **123**, 1262–1326.
9 T.-J. Yue, W.-M. Ren and X.-B. Lu, *Chem. Rev.*, 2023, **123**, 14038–14083.
10 C. E. Hoyle, A. B. Lowe and C. N. Bowman, *Chem. Soc. Rev.*, 2010, **39**, 1355.
11 A. Brändle and A. Khan, *Polym. Chem.*, 2012, **3**, 3224.
12 W.-M. Ren, T.-J. Yue, M.-R. Li, Z.-Q. Wan and X.-B. Lu, *Macromolecules*, 2017, **50**, 63–68.
13 J. Diebler, H. Komber, L. Häußler, A. Lederer and T. Werner, *Macromolecules*, 2016, **49**, 4723–4731.
14 Y. Wang, Y. Zhu, W. Lv, X. Wang and Y. Tao, *J. Am. Chem. Soc.*, 2023, **145**, 1877–1885.
15 T. Lee, P. T. Dirlam, J. T. Njardarson, R. S. Glass and J. Pyun, *J. Am. Chem. Soc.*, 2022, **144**, 5–22.
16 J. Chao, T. Yue, B. Ren, G. Gu, X. Lu and W. Ren, *Angew. Chem., Int. Ed.*, 2022, **61**, e202115950.
17 T. Tian, R. Hu and B. Z. Tang, *J. Am. Chem. Soc.*, 2018, **140**, 6156–6163.
18 J. Peng, T. Tian, S. Xu, R. Hu and B. Z. Tang, *J. Am. Chem. Soc.*, 2023, **145**, 28204–28215.
19 C. Zheng, H. Deng, Z. Zhao, A. Qin, R. Hu and B. Z. Tang, *Macromolecules*, 2015, **48**, 1941–1951.
20 P. Li, C. Tu, M.-M. Xun and W.-X. Wu, *Eur. Polym. J.*, 2022, **177**, 111482.
21 S.-Q. Wang, L.-H. Liu, K. Li, W. Xiong, H.-Z. Fan, Q. Cao, Z. Cai and J.-B. Zhu, *Polym. Chem.*, 2025, **16**, 987–993.
22 R. Sanaa, D. Portinha, R. Medimagh and E. Fleury, *Eur. Polym. J.*, 2024, **220**, 113498.
23 L. M. Lillie, W. B. Tolman and T. M. Reineke, *Polym. Chem.*, 2018, **9**, 3272–3278.
24 C. Li, W. Shi, D. Wu, M. Yang and Z. Xie, *Eur. Polym. J.*, 2023, **192**, 112065.
25 K. Bayram, B. Kiskan and Y. Yagci, *Polym. Chem.*, 2021, **12**, 534–544.
26 A. Hacioglu, V. Baddam, A. Kerr, J. Kehrein, A. Bunker and R. Luxenhofer, *Macromolecules*, 2024, **57**, 10368–10378.
27 H. J. Kim, D. W. Graham, A. A. DiSpirito, M. A. Alterman, N. Galeva, C. K. Larive, D. Asunskis and P. M. A. Sherwood, *Science*, 2004, **305**, 1612–1615.
28 K. B. Wiberg and P. R. Rablen, *J. Am. Chem. Soc.*, 1995, **117**, 2201–2209.
29 S. Behnken, T. Lincke, F. Kloss, K. Ishida and C. Hertweck, *Angew. Chem., Int. Ed.*, 2012, **51**, 2425–2428.
30 K. L. Dunbar, H. Büttner, E. M. Molloy, M. Dell, J. Kumpfmüller and C. Hertweck, *Angew. Chem.*, 2018, **130**, 14276–14280.
31 Y. Huang, Z. Cong, L. Yang and S. Dong, *J. Pept. Sci.*, 2008, **14**, 1062–1068.
32 I. Delfanne and G. Levesque, *Macromolecules*, 1989, **22**, 2589–2592.
33 W. Cao, F. Dai, R. Hu and B. Z. Tang, *J. Am. Chem. Soc.*, 2020, **142**, 978–986.
34 L. Huang and Q. Shuai, *ACS Sustainable Chem. Eng.*, 2019, **7**, 9957–9965.
35 A. Mathianaki, A. K. Demeler, A. Dömling, F. Ferrari, F. C. M. Scheelje, H. Bahmann and G. Delaittre, *Polym. Chem.*, 2025, **16**, 301–307.
36 M. Deletre and G. Levesque, *Macromolecules*, 1990, **23**, 4876–4878.
37 X. Yu, J. Jia, S. Xu, K. U. Lao, M. J. Sanford, R. K. Ramakrishnan, S. I. Nazarenko, T. R. Hoye, G. W. Coates and R. A. DiStasio, *Nat. Commun.*, 2018, **9**, 280.
38 Y. Shin, A. Welford, H. Komber, R. Matsidik, T. Thurn-Albrecht, C. R. McNeill and M. Sommer, *Macromolecules*, 2018, **51**, 984–991.
39 Y. Li, X. Zhang, H. Cheng, J. Zhu, S. Cheng and R. Zhuo, *Macromol. Rapid Commun.*, 2006, **27**, 1913–1919.
40 H. G. Schild, *Prog. Polym. Sci.*, 1992, **17**, 163–249.
41 K. Kubota, S. Fujishige and I. Ando, *Polym. J.*, 1990, **22**, 15–20.
42 I. Dimitrov, B. Trzebicka, A. H. E. Müller, A. Dworak and C. B. Tsvetanov, *Prog. Polym. Sci.*, 2007, **32**, 1275–1343.
43 K. Jain, R. Vedarajan, M. Watanabe, M. Ishikiriyama and N. Matsumi, *Polym. Chem.*, 2015, **6**, 6819–6825.
44 S. Nishimura, K. Nishida, T. Ueda, S. Shiomoto and M. Tanaka, *Polym. Chem.*, 2022, **13**, 2519–2530.
45 D. Jańczewski, N. Tomczak, M.-Y. Han and G. J. Vancso, *Eur. Polym. J.*, 2009, **45**, 1912–1917.
46 H. Zhang, T. Gao, L. Jiang, X. Meng, J. Wang, N. Ma, H. Wei and X. Zhang, *Eur. Polym. J.*, 2022, **173**, 111266.
47 J. Stephan, M. R. Stühler, C. Fornacon-Wood, M. Dimde, K. Ludwig, H. Sturm, J. L. Olmedo-Martínez, A. J. Müller and A. J. Plajer, *Polym. Chem.*, 2025, **16**, 1003–1009.
48 X. Yao, S. F. Zhang, N. Wei, L. W. Qian and S. Coseri, *Adv. Fiber Mater.*, 2024, **6**, 1256–1305.
49 X. Deng, R. A. Dop, D. Cai, D. R. Neill and T. Hasell, *Adv. Funct. Mater.*, 2024, **34**, 2311647.
50 J. M. Scheiger, C. Direksilp, P. Falkenstein, A. Welle, M. Koenig, S. Heissler, J. Matysik, P. A. Levkin and P. Theato, *Angew. Chem., Int. Ed.*, 2020, **59**, 18639–18645.
51 S. Wu, M. Luo, D. J. Darensbourg, D. Zeng, Y. Yao, X. Zuo, X. Hu and D. Tan, *ACS Sustainable Chem. Eng.*, 2020, **8**, 5693–5703.
52 R. G. Parr and R. G. Pearson, *J. Am. Chem. Soc.*, 1983, **105**, 7512–7516.

